Photodissociation to Several Atomic Terms: Near-threshold Resonance for Production of O(^{3}P) and O(^{1}D) in OH Photodissociation

Sungyul Lee

College of Environmental Science and Applied Chemistry, Kyunghee University, Kyungki-do 449-701, Korea
Received July 13, 2001

A theoretical analysis is presented for the multichannel type resonance at energies above the dissociation threshold to O(^{1}D) in the photodissociation of OH. Dissociations to both oxygenic terms O(^{3}P) and O(^{1}D) are treated. Total cross sections for producing these oxygen terms display asymmetric resonance due to the quantum interference resulting from complicated interplay of electronic states correlating to these two oxygenic terms. The branching ratios of O(^{3}P$_j$, j = 0, 1, 2), and the vector properties of O(^{3}P$_j$, j = 0, 1, 2) and O(^{1}D) display extensive changes near the threshold resonance as the result of the interactions among the electronic states correlated with O(^{3}P) and O(^{1}D).

Keywords : Photodissociation, Resonance, OH.

Introduction

Photodissociation[1] is a fundamental process that can provide ample dynamic information. Various kinds of interactions between the electronic states and quantum interference between the dynamic pathways may give extremely intriguing dynamic phenomena. In some simple situations, such as in direct dissociation, in which all the molecular electronic states correlated only with a single atomic term, measurements of the properties of photofragments such as the branching ratios and angular distributions may reveal direct information on the photoexcitation pathways and the symmetries of the electronically excited states.[2,3] In general situations, however, interplay of different kinds of interactions may complicate direct link between experimental observations and the mechanism of dynamic processes. Photodissociation to more than one atomic limit is such a case, because electronic states correlated with different atomic term limits may cross or experience avoided crossing in the Franck-Condon region. Loosely speaking, two kinds of non-Born-Oppenheimer interactions (first, the interactions, such as the spin-orbit coupling, between the crossing states correlated with different atomic terms in the Franck-Condon region, and second, the interactions in the asymptotic region between the electronic states correlating with the same atomic term) may influence the photodissociation processes in this situation. In this case, dynamics of photodissociation would be very different, depending on the energy regime considered. At energies *below* the threshold to the upper atomic term (O(^{1}D) in the present case), only lower term (O(^{3}P)) would be produced as we have shown in a series of publications.[4-7] since the electronic states correlating with the upper atomic term are *closed* channels. In many other studies on the predissociation processes, these latter states were neglected for good reasons.[8,9] At energies *above* the threshold to the upper atomic term, however, these molecular electronic states correlating with the upper atomic term must be explicitly included in the calculation, because these are *open* channels now. Any approximations for these states would fail to treat the production of the upper atomic term. Therefore, theoretical framework to deal with this general and complicated situation must certainly be needed to analyze experimental observations at energies *above* the threshold to the upper atomic term. This type of approach may also be a prelude to treating more complicated polyatomic processes, such as the photodissociation of CH_2BrCl[10] or CF_2Br_2[11] in energy regime from which two different atoms can be produced. To our best knowledge no investigations treated this interesting situation, properly including all the interactions discussed above to account for the complicated dynamics.

We describe in this work theoretical formalism to treat the production of two atomic terms in the photodissociation of diatomic molecules, and present calculations on the photodissociation of the OH molecule at energies above the dissociation threshold to O(^{1}D). We show that the theoretical method to treat the photodissociation process of OH below the threshold to O(^{1}D) may also be employed to compute for this more general situations. Productions of both O(^{1}D) and O(^{3}P) are theoretically treated. We predict the multichannel-type threshold resonance at these energies due to complicated interactions between the electronic states correlated with the two oxygenic terms, O(^{1}D) and O(^{3}P). Total cross sections for producing these oxygenic terms display the asymmetric resonance[12-17] peak due to the quantum interference, and the properties of O(^{1}D) and O(^{3}P) exhibit rapid changes near the resonance energies.

Theory and Computational Methods

We employ the theory[4] that can treat the very general situations in which there can be more than one atomic term limit involved and where there can be all kinds of crossings and avoided crossings among the electronic states. The theory was described in detail in Ref. 4, and we only briefly summarize it here to help present the results in Section III. Two basis sets are employed to describe the dissociation

dynamics in the molecular and asymptotic region, respectively. The first basis (ABO basis set) is a space-fixed one derived from Hund's coupling cases. Hund's case (a) basis is used here, although other coupling cases may also be employed as long as all the interactions are included to evaluate the total Hamiltonian. The second basis set $|J_F M j l j_O j_H>$, which is called the 'asymptotic' molecular basis, diagonalizes the total Hamiltonian at infinite internuclear distances. This basis is employed to properly describe the transition amplitudes for the dissociation to each atomic fine structure state of the oxygenic and hydrogenic terms with total electronic angular momentum quantum numbers j_O and j_H, respectively. Here, l is the orbital angular momentum quantum number, $j = j_O + j_H$, and J_F ($= j + l$) is the total final angular momentum quantum number. M is the z component of J_F in the space-fixed coordinate system. These two basis sets are related to each other by the r-independent transformation matrix $<jlj_O j_H \quad C\Lambda S\Sigma p>_J$. The scattering equation,

$$[E-H]|\, k, j_O m_O j_H m_H^{(+)}\rangle = 0, \tag{1}$$

is solved, where H is the full Hamiltonian which describes motion on the excited states and k is the wave vector. The scattering wave function $|\, k, j_O m_O j_H m_H^{(+)}\rangle$ is expanded in terms of energy-normalized continuum eigenfunction $|\, EJ_F M j l j_O m_O j_H m_H^{(+)}\rangle$ of the total angular momentum operator J_F

$$|\, k, j_O m_O j_H m_H^{(+)}\rangle = \sum_{J_F l m \mu} |EF_F M j l j_O j_H^{(+)}\rangle \langle J_F M \,|\, j l m \mu\rangle \times \langle jm \,|\, j_O j_H m_O m_H\rangle i^l Y_{l\mu}^{*}. \tag{2}$$

Close-coupled equations are solved to obtain the continuum wave function $|\, EJ_F M j l j_O m_O j_H m_H^{(+)}\rangle$. Transition amplitudes to a specific fine structure component of the oxygen atom are computed by the Golden Rule, and can be factored using the Wigner-Eckart theorem to separate the dependence on M_i, M

$$T(k, j_O j_H \,|\, i) = \sum_{J_F l m \mu} \langle EJ_F M j l j_O j_H^{(+)} | \hat{\varepsilon} \cdot x | J_i M_i \eta_i\rangle$$

$$= \sum_{q} \langle j_F M \,|\, 1 J_i q M_i\rangle \varepsilon_q^{*} \tau(J_F j l j_O j_H | J_i \eta_i), \tag{2}$$

where $|\, J_i M_i \eta_i>$ is the wave function for the initial state, and $\tau(J_F j l j_O j_H \,|\, J_i \eta_i)$ is called the reduced transition amplitude. The double differential cross section for the coincidence detection of photofragments and fluorescence is obtained as

$$\frac{d^2\sigma}{d\Omega_\varepsilon d\Omega_k}(\hat{\varepsilon}_s, \hat{k}) = \sum_{K_S Q_S K_D Q_D} \sigma_{K_S Q_S K_D Q_D} \phi_{K_S Q_S}(\hat{\varepsilon}_s) C_{K_D Q_D}(\hat{k}). \tag{4}$$

where ε_S is the polarization vector, relative to the space-fixed (SF) z-axis, of the emitted light from an excited photofragment. The vector properties of the photodissociation processes are given in terms of the ratios of σ's, which are described in Ref. 3 in terms of the geometrical factor and the dynamical τ factor. C_{KQ} is the renormalized spherical harmonics, and ϕ is the photon polarization density matrix defined by

$$\phi_{K_S Q_S}(\hat{\varepsilon}_s) = \sum_{q\bar{q}} (-1)^{1-\bar{q}} \langle K_S Q_S \,|\, 11 q - \bar{q}\rangle \varepsilon_q \varepsilon_{\bar{q}}^{*}. \tag{5}$$

The integral cross section for dissociation to a particular spin-orbit component of the fragment atom is obtained as

$$\sigma_{00,00} = \frac{4\pi^2 \alpha\omega}{3} \frac{1}{2J_i + 1} \sum_{J_F l} (2J_F + 1) |\, \tau(J_F j l j_O j_H | J_i \eta_i)|^2. \tag{6}$$

The fragment anisotropy parameter (for the angular distributions) and the alignment parameter are obtained as the ratio of the partial cross sections

$$\beta_D = \frac{\sigma_{00:20}}{\sigma_{00,00}} \tag{7}$$

and

$$\beta_S = \frac{\sigma_{02:00}}{\sigma_{00,00}} \tag{8}$$

respectively (the definitions of σ's included in these equations are given in Ref. 3).

The propagation of the scattering wave function is carried out by the Renormalized Numerov method.[18] and appropriate boundary conditions are imposed at the end of propagation (up to 25 bohr). Convergence of the computed results is confirmed by increasing the number of integration steps up to 2500. The potential curves, transition dipole moments and the spin-orbit couplings employed in the present calculations were described in Ref. 4.

Results

Figure 1 depicts the potential curves of the electronic states included in the present calculations. Zero of the energy is defined as the statistical average of the energy splittings of $O(^3P_j, j = 0, 1, 2)$ in Figure 1. The $X^2\Pi$, $^4\Sigma^-$, $^2\Sigma^-$ and $^4\Pi$ states correlate with $O(^3P)$, while the $A^2\Sigma^+$, $^2\Delta$ and $2^2\Pi$ states

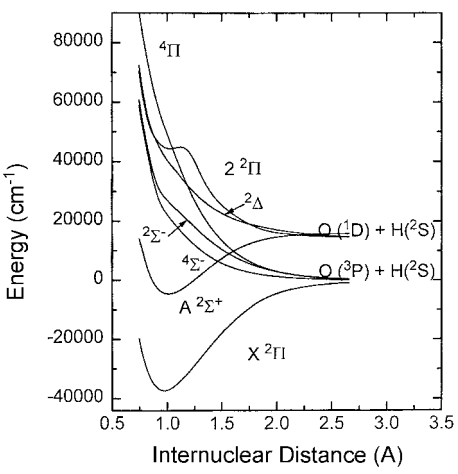

Figure 1. *Ab initio* Potential energy curves of OH. Zero of the energy is defined as the baricenter of the energies of $O(^3P_j, j = 0, 1, 2)$.

correlate with $O(^1D)$. At energies between thresholds to $O(^3P)$ and $O(^1D)$, the dynamics is described as predissociation of the $A^2\Sigma^+$ state by the three dissociative $^4\Sigma^-$, $^2\Sigma^-$ and $^4\Pi$ states,[4-7] resulting from the spin-orbit couplings of this state with the three repulsive $^4\Sigma^-$, $^2\Sigma^-$ and $^4\Pi$ states. Since both of the bound $A^2\Sigma^+$ and dissociative $^2\Sigma^-$ state are optically coupled with the ground $X^2\Pi$ state, and since these two excited states interact by spin-orbit couplings, absorption spectrum in this energy regime may exhibit asymmetric resonance line shapes as a result of the quantum interference between two indistinguishable pathways: that is, between the three indirect dissociation paths *via* the $A^2\Sigma^+$ state and the direct path *via* the $^2\Sigma^-$ state.

At energies above the threshold to dissociation to $O(^1D)$, the photodissociation dynamics may become much more complicated for several reasons. First, the channels for the $O(^1D)$ term are now open, and dissociations both to $O(^3P)$ and $O(^1D)$ compete at these energies. Second, the electronic states ($A^2\Sigma^+$, $^2\Delta$ and $2^2\Pi$) correlating with $O(^1D)$ play a significant role in the dynamics, and interactions among them would affect the properties of $O(^1D)$ produced. Third, interactions among these states correlating with $O(^1D)$ and those ($X^2\Pi$, $^4\Sigma^-$, $^2\Sigma^-$ and $^4\Pi$) correlating with $O(^3P)$ may also affect the outcomes of photodissociation in a complicated fashion. For example, these interactions may give rise to the multichannel-type resonance at energies near the threshold to $O(^1D)$. The effects of quantum interference may influence the resonances for production of $O(^3P)$ and $O(^1D)$ in different ways. More specifically, the degree of asymmetry of the resonances would be different. In this work, we show that the interactions among the electronic states correlating with $O(^3P)$ or $O(^1D)$ can yield threshold resonances at energies above the dissociation limit to $O(^1D)$ both for dissociation to $O(^3P)$ and $O(^1D)$.

Figure 2 shows such resonances reached from the initial ground $X^2\Pi^+_{2/3}$ state (J_i = 15.5 and v_i = 0). In the total cross section for producing $O(^3P_j, j = 0, 1, 2)$, two resonances are observed at E = 15880 and 15908 cm^{-1}. These resonances

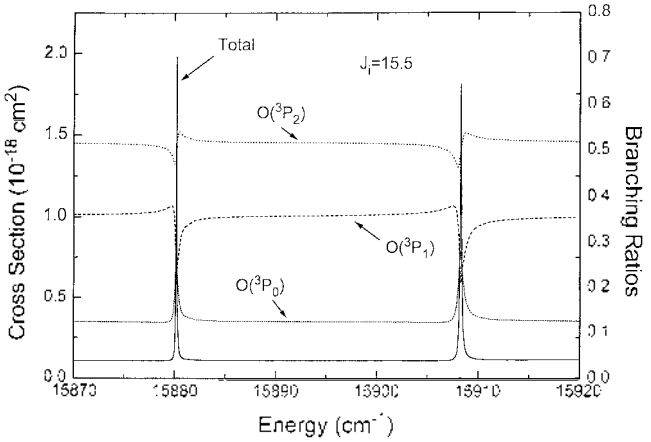

Figure 2. Multichannel threshold resonances lying above the threshold to $O(^1D)$, reached from the initial ground $X^2\Pi^+_{2/3}$ state (J_i = 11.5 and v_i = 0). Total cross section and branching ratios for production of $O(^3P_j, j = 0, 1, 2)$.

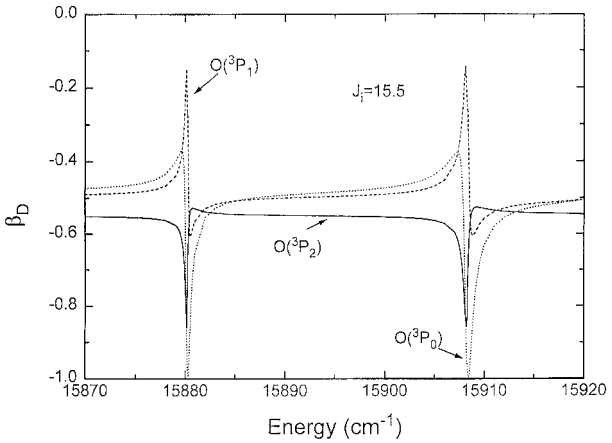

Figure 3. Anisotropy parameters β_D of angular distributions of $O(^3P_j, j = 0, 1, 2)$.

exhibit asymmetric features.[12-17] The asymmetry of the two resonances can be seen more clearly by noticing that the branching ratios for production of $O(^3P_j, j = 0, 1, 2)$ changes considerably near the resonances in Figure 2. Figure 3 depicts the angular distribution anisotropy parameters[19-21] β_D of $O(^3P_j, j = 0, 1, 2)$ near the resonance. The values of β_D are different from each other, and they change rapidly near the resonance. Different values of β_D's for $O(^3P_j, j = 0, 1, 2)$ near the resonance suggests that angular resolution of photofragments may be possible near the multichannel resonance. It is noteworthy to observe that the values of β_D of about 0.5 are different from the high-energy recoil limit value (−1) for perpendicular ($|\Delta\Omega| = 1$, $\Pi \leftarrow \Sigma$) electronic transition at off-resonance energies. It seems that both of the perpendicular transitions ($A^2\Sigma^- \leftarrow X^2\Pi$ and $^2\Sigma^- \leftarrow X^2\Pi$) may interfere to affect the angular distributions of $O(^3P_j, j = 0, 1, 2)$. The fluorescence anisotropy parameters[2,3] β_S of $O(^3P_j, j = 0, 1, 2)$ shown in Figure 4 also exhibit similar behaviors near the resonance. The dissociation to $O(^1D)$ is also open at energies near these resonances, and the spectrum for dissociation to this state of the oxygen atom is given in Figure 5 along with the values of β_D and β_S. The cross section at the

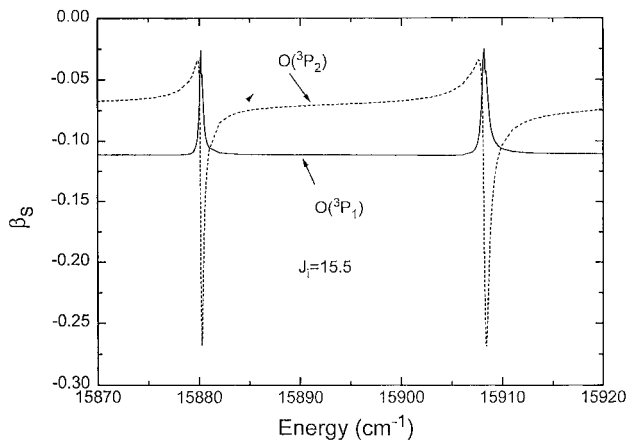

Figure 4. Fluorescence anisotropy parameters β_S of $O(^3P_j, j = 0, 1, 2)$.

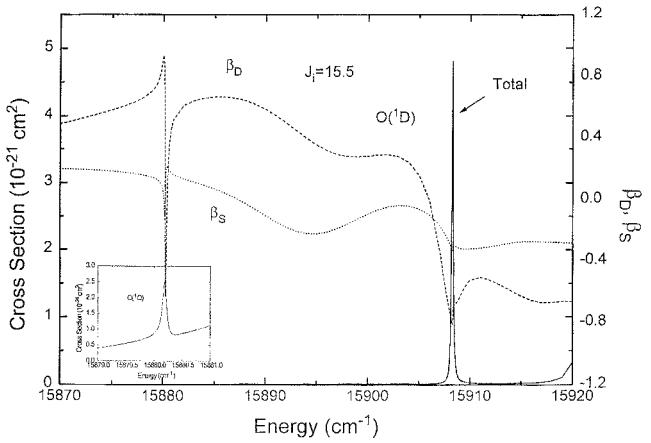

Figure 5. Total cross section and anisotropy parameters β_D and β_S for production of O(^{1}D).

resonance at E = 15880 cm^{-1} is so much smaller than that at E = 15908 cm^{-1} that it is included as inset. Both anisotropy parameters β_D and β_S display rapid changes near the resonances. The asymmetry of the resonance E = 15880 cm^{-1} is now very evident. The computed asymmetry of the resonance and the rapid changes of the vector properties near the resonance could give useful information when they are compared with the experimentally measured values. Specifically, the interactions between the bound and the dissociative states, and the relative oscillator strengths from the initial state to the bound and the dissociative states could be determined by direct computation of the asymmetry parameters as shown in our previous work.[24]

Since the resonances shown in Figure 2-Figure 5 lie above the threshold to O(^{1}D), they do not correspond to the rovibrational levels of the $A^2\Sigma^+$ state. They rather seem to correspond to the shape resonance attributable to the centrifugal barrier of the dissociative states. Since the height of the centrifugal barrier depends on the magnitude of the orbital angular momentum quantum number l for the relative motion of the two nuclei, and since $J_F = j + l$, there would hardly be resonances observed for low J_F, if the multichannel resonances are due to the centrifugal barrier. Therefore we carry out the computations for low J_F, say J_F = 1.5, and confirm that indeed no multichannel-type resonance is computed. These resonances are, however, different from ordinary shape resonance, since the effects of the asymptotic interactions are also seen. For example, it should be noted that the resonances are seen both in the cross section for dissociation to O(^{3}P) and to O(^{1}D) in Figure 2. If the resonance is due to the centrifugal barrier of only one of the dissociative states, cross sections for dissociation to O(^{3}P) or to O(^{1}D) would exhibit resonance. Therefore, it seems to be of multichannel character, as shown by Freed and co-workers for the threshold resonances in the photodissociation of CH^-.[2]

Since these resonances are predicted to be observed just above the threshold to the upper atomic term O(^{1}D), the kinetic energy of the atoms produced is small. Thus, these resonances would correspond to those observed in the collision of ultracold atoms.[22,23] The multichannel resonances predicted in this work in the photodissociation of OH, therefore, may also be observed in the collision of ultracold O(^{1}D) and H(^{2}S) atoms. Experimental study on this type of multichannel threshold resonances will be very intriguing.

Acknowledgment. This work was supported by Korea Science and Engineering Foundation Grant (1999-1-121-001-5).

References

1. Schinke, R. *Photodissociation Dynamics*; Cambridge University Press: Cambridge, 1993.
2. (a) Williams, C. J.; Freed, K. F.; Singer, S. J.; Band, Y. B. *Far. Disc. Chem. Soc.* **1986**, *82*, 1. (b) Williams, C. J.; Freed, K. F. *J. Chem. Phys.* **1986**, *85*, 2699.
3. (a) Singer, S. J.; Freed, K. F.; Band, Y. B. *Adv. Chem. Phys.* **1985**, *61*, 1. (b) Singer, S. J.; Freed, K. F.; Band, Y. B. *J. Chem. Phys.* **1983**, *79*, 6060.
4. Lee, S. *J. Chem. Phys.* **1995**, *103*, 3501.
5. (a) Lee, S. *Bull. Korean Chem. Soc.* **1995**, *16*, 387; *Chem. Phys. Lett.* **1995**, *240*, 595. (b) *J. Phys. Chem.* **1995**, *99*, 13380; *Bull. Korean Chem. Soc.* **1995**, *16*, 801.
6. Lee, S. *J. Chem. Phys.* **1996**, *104*, 1912; **1999**, *111*, 6407.
7. Lee, S. *Chem. Phys. Lett.* **1995**, *243*, 250; *J. Chem. Phys.* **1996**, *105*, 10782; **1997**, *107*, 1388; *Phys. Rev.* **1996**, *A54*, R4621; **1998**, *58*, 4981.
8. Yarkony, D. R. *J. Chem. Phys.* **1992**, *97*, 1838.
9. Parlant, G.; Yarkony, D. R. *J. Chem. Phys.* **1999**, *110*, 363.
10. Lee, S.-H.; Jung, Y.-J.; Jung, K.-H. *Chem. Phys.* **2000**, *260*, 143.
11. Park, M.-S.; Kim, T. K.; Lee, S.-H.; Jung, K.-H.; Volpp, H.-R.; Wolfrum, J *J. Phys. Chem. A* **2001**, *105*, 5606.
12. Fano, U. *Phys. Rev.* **1961**, *61*, 1866.
13. Kim, B.; Yoshihara, K.; Lee, S. *Phys. Rev. Lett.* **1994**, *73*, 424.
14. Lee, S.; Sun, H.; Kim, B.; Freed, K. F. *J. Chem. Phys.* **2001**, *114*, 5537.
15. Glass-Maujean, M.; Breton, J.; Guyon, P. M. *Chem. Phys. Lett.* **1979**, *63*, 591.
16. Brandon, J. T.; Reid, S. A.; Robie, D. C.; Reisler, H. *J. Chem. Phys.* **1992**, *97*, 5246.
17. Lewis, B. R.; Banerjee, S. S.; Gibson, S. T. *J. Chem. Phys.* **1995**, *102*, 6631.
18. Johnson, B. R. *J. Chem. Phys.* **1977**, *67*, 4086.
19. Seideman, T. *J. Chem. Phys.* **1995**, *103*, 10556.
20. Wang, J. W.; Kleiber, P. D.; Sando, K. M.; Stwalley, W. C. *Phys. Rev. A* **1990**, *42*, 5352.
21. Greene, C. H.; Zare, R. N. *Annu. Rev. Phys. Chem.* **1982**, *33*, 119; *J. Chem. Phys.* **1983**, *78*, 6741.
22. Lett, P. D.; Julienne, P. S.; Phillips, W. D. *Annu. Rev. Phys. Chem.* **1995**, *46*, 423.
23. Wang, H.; Wang, X. T.; Gould, P. L.; Stwalley, W. C. *Phys. Rev. Lett.* **1997**, *78*, 4173.
24. Lee, S.; Kim, B. *J. Phys. B* **2000**, *33*, 3441.